Homophilic adhesion and CEACAM1-S regulate dimerization of CEACAM1-L and recruitment of SHP-2 and c-Src

Mario M. Müller,[1] Esther Klaile,[1] Olga Vorontsova,[1] Bernhard B. Singer,[2] and Björn Öbrink[1]

[1]Department of Cell and Molecular Biology, Karolinska Institutet, 171 77 Stockholm, Sweden
[2]Department of Anatomy, University Hospital Essen, 45147 Essen, Germany

Carcinoembryonic antigen (CEA)–related cell adhesion molecule 1 (CAM1 [CEACAM1]) mediates homophilic cell adhesion and regulates signaling. Although there is evidence that CEACAM1 binds and activates SHP-1, SHP-2, and c-Src, knowledge about the mechanism of transmembrane signaling is lacking. To analyze the regulation of SHP-1/SHP-2/c-Src binding, we expressed various CFP/YFP-tagged CEACAM1 isoforms in epithelial cells. The supramolecular organization of CEACAM1 was examined by cross-linking, coclustering, coimmunoprecipitation, and fluorescence resonance energy transfer. SHP-1/SHP-2/c-Src binding was monitored by coimmunoprecipitation and phosphotyrosine-induced recruitment to CEACAM1-L in cellular monolayers. We find that trans-homophilic CEACAM1 binding induces cis-dimerization by an allosteric mechanism transmitted by the N-terminal immunoglobulin-like domain. The balance of SHP-2 and c-Src binding is dependent on the monomer/dimer equilibrium of CEACAM1-L and is regulated by trans-binding, whereas SHP-1 does not bind under physiological conditions. CEACAM1-L homodimer formation is reduced by coexpression of CEACAM1-S and modulated by antibody ligation. These data suggest that transmembrane signaling by CEACAM1 operates by alteration of the monomer/dimer equilibrium, which leads to changes in the SHP-2/c-Src–binding ratio.

Introduction

Cell adhesion molecules (CAMs) signal across the plasma membrane to process information from the extracellular environment. The mechanism of information transfer across the plasma membrane is known in some detail for integrins, which are heterodimeric transmembrane proteins (for review see Luo et al., 2007). However, our knowledge about transmembrane signaling mechanisms by homophilic cell–CAMs consisting of single polypeptide chains, such as cadherins and immunoglobulin-like (Ig) CAMs, is limited. Insights into these processes are important not only for understanding basic cell biological behavior, but also because it has great impact on several medical and pathological conditions such as cancer, infection, and inflammation. The focus of this study is to provide information on the mechanism and regulation of transmembrane signaling by a class of homophilic Ig CAMs.

One subfamily within the Ig CAM superfamily is the carcinoembryonic antigen (CEA) family (Öbrink, 1997; Beauchemin et al., 1999), which plays important roles in a variety of cell-based events, including morphogenesis (Yokoyama et al., 2007), vasculogenesis (Gu et al., 2009), angiogenesis (Horst et al., 2006), cell proliferation (Scheffrahn et al., 2005), cell motility (Klaile et al., 2005; Müller et al., 2005), apoptosis (Kirshner et al., 2003; Singer et al., 2005), tumor growth (Leung et al., 2008), invasion (Ebrahimnejad et al., 2004), infection, and inflammation (Gray-Owen and Blumberg, 2006). The primordial molecule in the CEA family is CEA-related CAM1 (CEACAM1), a single-pass transmembrane type I glycoprotein, which is expressed as differentially spliced isoforms (Öbrink, 1997; Gray-Owen and Blumberg, 2006). The two major isoforms that differ only in their cytoplasmic domains but have identical transmembrane

Correspondence to Björn Öbrink: bjorn.obrink@ki.se

Abbreviations used in this paper: CAM, cell adhesion molecule; CEA, carcinoembryonic antigen; CEACAM1, CEA-related CAM1; FRET, fluorescence resonance energy transfer; Ig, immunoglobulin like; ROI, region of interest; shRNA, short hairpin RNA.

The Rockefeller University Press $30.00
J. Cell Biol. Vol. 187 No. 4 569–581
www.jcb.org/cgi/doi/10.1083/jcb.200904150

domains and ectodomains consisting of four Ig domains are CEACAM1-4L and CEACAM1-4S. In most CEACAM1-expressing cell types, CEACAM1-4L and CEACAM1-4S are coexpressed, albeit at different ratios in different cell types (Singer et al., 2000; Gaur et al., 2008). In CEACAM1-L, two phosphorylatable tyrosine residues play an important role in signaling. Upon phosphorylation, these tyrosine-based sequences can bind and activate the cytoplasmic protein tyrosine phosphatases SHP-1/SHP-2 (Huber et al., 1999) and Src family tyrosine kinases (Brümmer et al., 1995). Recent studies have implicated these enzymes, which compete for the same phosphotyrosine-binding sites as major effectors in CEACAM1-L–mediated signaling (Boulton and Gray-Owen 2002; Singer et al., 2005; Nagaishi et al., 2006; Slevogt et al., 2008).

CEACAM1 signal regulation is influenced by its adhesion-mediating homophilic trans-binding activity (Gray-Owen and Blumberg, 2006). However, the nature of the transmembrane signal that is triggered by the trans-homophilic binding is unknown. We have suggested that it involves changes in the dimerization state (Öbrink et al., 2002) and have recently been able to show that trans-homophilic binding between membrane-attached CEACAM1 ectodomains indeed increases cis-dimerization (see Klaile et al. on p. 553 of this issue). In this study, we set out to investigate whether a similar mechanism operates in the plasma membrane of viable epithelial cells. The results demonstrate that transmembrane signaling by CEACAM1-L is a function of its lateral interactions, which determine the binding proportions of SHP-1, SHP-2, and c-Src to the CEACAM1-L cytoplasmic domains. The state of the CEACAM1-L supramolecular organization is regulated both by CEACAM1 trans-homophilic cell adhesion and by the expression level of CEACAM1-S and can be modulated by antibodies.

Results

Silencing and reexpression of CEACAM1 in NBT-II cells

NBT-II cells were chosen because they express endogenous CEACAM1 and contain an appropriate response machinery for CEACAM1-mediated signal regulation (Scheffrahn et al., 2005). To express reporter-labeled CEACAM1 isoforms, endogenous CEACAM1 was permanently down-regulated by stable transfection with a vector coding for a short hairpin RNA (shRNA) targeting exon 9. In the most efficiently down-regulated clones, endogenous CEACAM1 was undetectable by cytofluorimetry (not depicted) or Western blotting, and other CAMs such as α3 and α6 integrins and E-cadherin were unaffected (Fig. S1 A). One clone, C2Dc3, was chosen for further experiments.

In addition to full-length CEACAM1-4L and CEACAM1-4S, two truncated CEACAM1 molecules were reexpressed in C2Dc3 cells, namely ΔN–CEACAM1-3L and CEACAM1-4ΔCyto, which lacked the N-terminal Ig domain (D1) or the cytoplasmic domain, respectively. To allow monitoring and fluorescence resonance energy transfer (FRET) analysis, monomeric CFP or YFP (Kim et al., 2003) was inserted between the fourth Ig domain (D4) and the transmembrane domain in all of the constructs (Fig. 1 A).

Cell surface expression of all CEACAM1 constructs was verified by cytofluorimetry (unpublished data). Immunoprecipitation and Western blots of cellular lysates showed expression of a major band, corresponding to the size of wild-type CEACAM1 plus that of CFP/YFP and a smaller minor band for all CEACAM1 constructs (Fig. S1 B). Both bands reacted with anti-CEACAM1 and anti-GFP antibodies, suggesting that the smaller band represents an underglycosylated form. This isoform was apparently not expressed at the cell surface because it was not accessible for cross-linking in intact cells by a water-soluble cross-linking agent (Fig. 1 B).

Confocal microscopy demonstrated that the CEACAM1-4L–YFP/CFP and CEACAM1-4S–YFP/CFP constructs became localized to cell contact areas in a pattern indistinguishable from that of wild-type CEACAM1 (Fig. S1 C). Also, ΔN–CEACAM1-3L–YFP and CEACAM1-4ΔCyto–YFP became localized to cell contact areas. Cotransfection of CEACAM1-4L–YFP and CEACAM1-4S–CFP resulted in a complete codistribution of the two isoforms (Fig. S1 D).

Back-transfected CEACAM1 isoforms are functionally active

To investigate whether the reexpressed YFP/CFP-tagged CEACAM1 isoforms were functionally active, we analyzed their ability to mediate homophilic adhesion. C2Dc3 cells expressing CEACAM1-4L–YFP, CEACAM1-4S–YFP, and CEACAM1-4ΔCyto–YFP but not ΔN–CEACAM1-3L–YFP adhered efficiently only to surfaces coated with rat CEACAM1-Fc (Fig. S2 A). The adhesion mediated by CEACAM1-4L–YFP/CEACAM1-4S–YFP/CEACAM1-4ΔCyto–YFP and wild-type CEACAM1 required FBS and was partially inhibited by the tyrosine kinase inhibitor PP2 and strongly inhibited by the SHP-1/SHP-2 inhibitor NSC-87877 (Fig. S2 B). The inhibitors did not alter the surface expression of CEACAM1 (Fig. S2 D) or the cell viability because adhesion to collagen I was not affected (Fig. S2 C). These results show that the reexpressed CFP/YFP-tagged CEACAM1 isoforms were functionally active and that homophilic cell adhesion by CEACAM1 is an active process regulated by intracellular signaling events.

Supramolecular organization of CEACAM1 in the plasma membrane

Previous work has demonstrated that endogenous CEACAM1 can form cross-linkable dimers in the plane of the plasma membrane (Hunter et al., 1996). Cross-linking of the back-transfected cells with a water-soluble cross-linker showed that all YFP-tagged isoforms of CEACAM1 appeared as a mixture of monomers, a significant proportion of dimers, and a small fraction of larger oligomers, which is comparable with wild-type CEACAM1 (Fig. S1 E). Similar levels of cross-linked dimers occurred in both adherent, contacting cells, and in suspended single cells (Fig. 1 B), suggesting that the stabilized dimers represented cis-dimers. This was directly demonstrated by the finding that trans-dimers were not stabilized by cross-linking as determined in an experiment in which cells expressing wild-type CEACAM1 and CEACAM1-4LΔCyto–YFP were mixed, allowed to adhere to each other, and subjected to cross-linking. No YFP reactivity

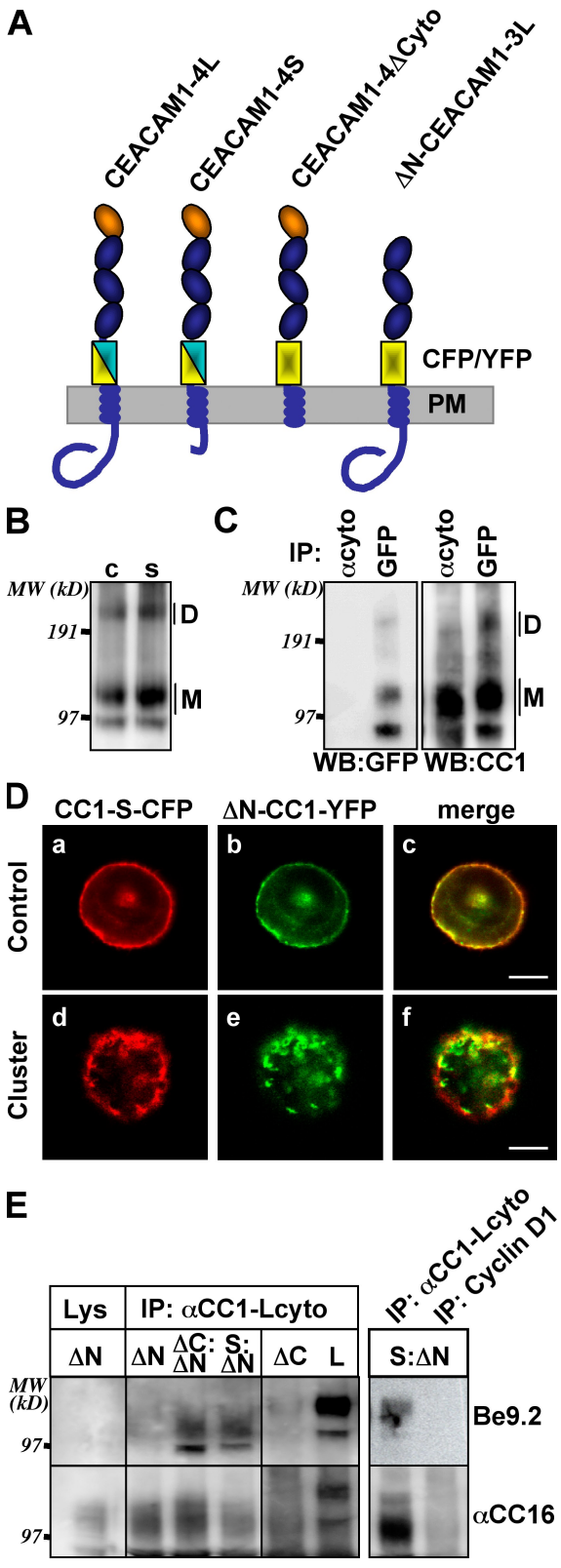

Figure 1. **Homophilic CEACAM1 cis-interactions in the plasma membrane.** (A) Graphic representation of reexpressed CEACAM1 isoforms/mutants in C2Dc3 cells. CFP (blue) or YFP (yellow) was inserted between the membrane proximal Ig domain and the transmembrane domain. (B) Cross-linking of CEACAM1-4L–YFP in confluent monolayer (c) and suspended (s) cells with BS^3. M, monomer; D, dimer. (C) Wild-type NBT-II cells expressing CEACAM1-S and CEACAM1-L were cocultured with CEACAM1-4ΔCyto–YFP-expressing cells at a 3:1 ratio, grown to confluence, and cross-linked. CEACAM1-L was immunoprecipitated either with anti–cytoplasmic domain (αcyto) or anti-GFP antibodies. The immunoprecipitates were analyzed for GFP reactivity (left) or CEACAM1 reactivity (right) by Western blotting (WB). No GFP immunoreactivity was detected in the CEACAM1-L precipitates, even after prolonged exposure on x-ray films. (D) CEACAM1-4S–CFP-expressing cells were transiently transfected with ΔN–CEACAM1-3L–YFP and seeded on poly-L-lysine–coated coverslips. CC1-S-CFP was clustered with mAb 5.4 and goat anti–mouse antibodies. The cells were fixed and analyzed for the distribution of CC1-S-CFP (a and d, red) and ΔN-CC1-YFP (b and e, green). Merged images (c and f) show coclustering (yellow) of the two CEACAM1 isoforms. Bars, 10 μm. (E) Lysates of C2Dc3 cells expressing CEACAM1-4ΔCyto–YFP (ΔC), ΔN–CEACAM1-3L–YFP (ΔN), or coexpressing CEACAM1-4S–YFP/ΔN–CEACAM1-3L–YFP (S:ΔN) or CEACAM1-4ΔCyto–YFP/ΔN–CEACAM1-3L–YFP (ΔC:ΔN) were immunoprecipitated with CEACAM1-L cytoplasmic domain–specific antibodies. (top) N domain–containing CEACAM1 molecules in complex with L-cytoplasmic domain–containing proteins were detected by immunoblotting with mAb Be9.2. (bottom) Filters were reprobed with αCC16 for detection of precipitated CEACAM1. (right) Immunoprecipitation with anti–cyclin D1 was used as rabbit IgG control. IP, immunoprecipitation; MW, molecular weight.

was detected by immunoprecipitation with an anti–L-cytoplasmic domain antibody (Fig. 1 C).

To collect further information on the nature of cis-dimerization, two additional sets of experiments were performed. In one experiment, silenced cells were cotransfected with CEACAM1-4S–CFP and ΔN–CEACAM1-3L–YFP. CEACAM1-4S–CFP was clustered with mAb 5.4 (directed against the N-terminal domain) and secondary antibodies. This resulted in coclustering of ΔN–CEACAM1-3L–YFP (Fig. 1 D). In the other experiment, silenced cells were cotransfected with either CEACAM1-4S–CFP and ΔN–CEACAM1-3L–YFP or CEACAM1-4ΔCyto–YFP and ΔN–CEACAM1-3L–YFP. Immunoprecipitation with the anti–L-cytoplasmic domain antibody, recognizing ΔN–CEACAM1-3L–YFP, resulted in coprecipitation of CEACAM1-4S–CFP and CEACAM1-4ΔCyto–YFP (Fig. 1 E). Both experiments demonstrate that CEACAM1 molecules can interact with each other in cis through Ig domains D2–D4 and/or via their transmembrane domains.

Characterization of CEACAM1 cis-interactions by FRET

Cis-interactions of CEACAM1 were further analyzed by FRET microscopy. Acceptor photobleaching was used to measure FRET both in contact regions and free edges of cells attached to poly-L-lysine–coated glass coverslips (Fig. 2 A). Insignificant FRET signals (FRET efficiency [E] = 0.60 ± 0.96%) were observed in contacts between cells that were monotransfected with CEACAM1-4L–CFP and CEACAM1-4L–YFP, demonstrating that the observed FRET in cotransfected cells emanated from cis-interactions in the plane of the plasma membrane and not from adhesion-mediating CEACAM1 in trans.

Efficient FRET at cell edges was observed with CEACAM1-4L/CEACAM1-4L, CEACAM1-4S/CEACAM1-4S, and CEACAM1-4L/CEACAM1-4ΔCyto combinations (Fig. 2 B). Pairs of ΔN–CEACAM1-3L/CEACAM1-4L and ΔN–CEACAM1-3L/CEACAM1-4S exhibited strikingly lower FRET efficiencies (Fig. 2 B), showing that the N-terminal Ig domain has an important and dominating role in these cis-interactions,

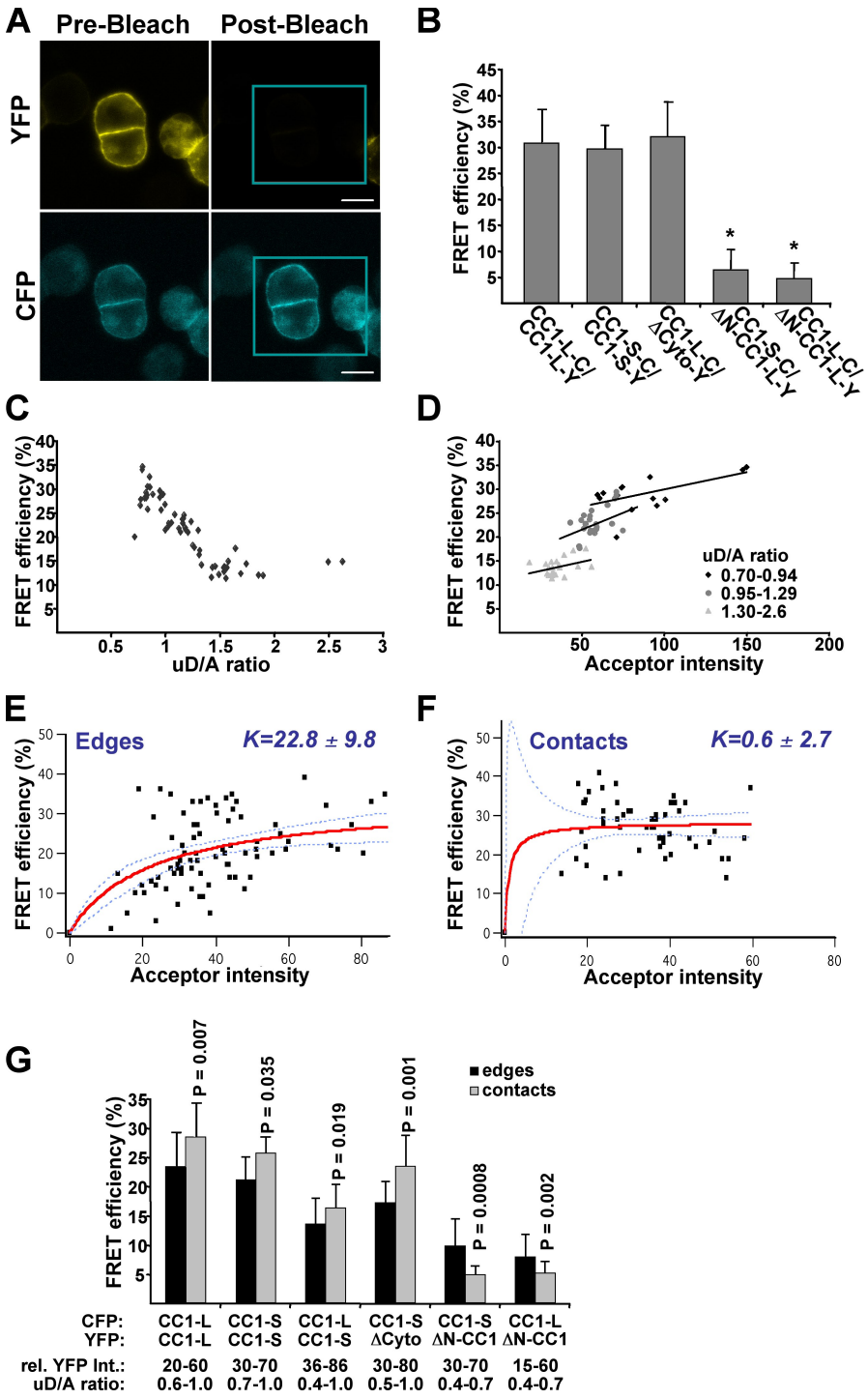

Figure 2. **CEACAM1 cis-interactions determined by FRET.** (A) Images of CFP and YFP fluorescence of contacting cells expressing CEACAM1-4L–CFP and CEACAM1-4L–YFP before and after YFP bleaching. Note the disappearance of YFP fluorescence and increase of CFP fluorescence (in the boxed areas) after bleaching. Bars, 10 µm. (B) FRET efficiencies (mean ± SD) in free cell edges of the indicated pairs of coexpressed CEACAM1 isoforms at a 0.6–1.0 uD/A ratio and acceptor intensity of 80–110. *, $P < 0.0001$ (Student's *t* test). (C) FRET efficiency plotted versus uD/A ratio for free edges of cells expressing CEACAM1-4S–CFP/CEACAM1-4S–YFP ($n = 14$; four ROIs per cell). (D) FRET efficiency plotted versus acceptor fluorescence at different uD/A ratios for the same 14 cells as in C. (E and F) FRET in free cell edges (E) and contact regions (F) for CEACAM1-4L–CFP/CEACAM1-4L–YFP-expressing cells at a 0.6–1.0 uD/A ratio. The least-square fits of the experimental data to Eq. 1 are shown as red curves with 95% confidence intervals shown as flanking blue curves. The fitted value for K ± SD is shown for each graph. (G) Comparison of FRET efficiencies at free edges and contact regions for similar pairs of coexpressed CEACAM1 as in B. The uD/A ratios, acceptor intensity ranges, and p-values (Student's *t* test) are shown for each pair.

whereas the cytoplasmic domains do not contribute significantly. The FRET efficiency of CEACAM1-4L/CEACAM1-4L (not depicted) and CEACAM1-4S/CEACAM1-4S in the free cell edges decreased with increasing uD/A (postbleach CFP intensity/prebleach YFP intensity) ratios (Fig. 2 C). Plotting the FRET efficiency against acceptor fluorescence intensity at different uD/A ratios showed decreasing FRET efficiency with an increasing uD/A ratio (Fig. 2 D). Furthermore, at a given uD/A ratio, the FRET efficiency in the free cell edges increased smoothly and showed a curvy linear dependence on acceptor density (Fig. 2 E). According to current FRET theory (Kenworthy and Edidin, 1998; Zacharias et al., 2002), these results show that CEACAM1-4L and CEACAM1-4S occur as mixtures of randomly distributed monomers and specifically microclustered cis-dimers and/or small cis-oligomers in the free cell edges.

The FRET signals were different in the cell contact regions. In contrast to the behavior in free cell edges, there was no dependence on the acceptor density (Fig. 2 F). This relationship of FRET efficiency and acceptor intensity has been expressed as a saturable one-site binding model,

$$E = E_{max} \times F/(F + K), \quad (1)$$

where E is a hyperbolic function of the cell surface density (F), and K is analogous to a dissociation constant of the microclusters (Zacharias et al., 2002). A K value can be obtained by curve fitting of the FRET data to Eq. 1. However, the obtained K does not represent a true dissociation constant, especially because the data represent a mixture of different proportions of randomly distributed molecules and microclusters. Nevertheless, K values obtained under different conditions can be compared with yield information on the tendency to form microclusters; the lower the K value, the greater the tendency to cluster. Fitting of the data in Fig. 2 (E and F) yielded a drastically lower K value for FRET in cell contacts compared with FRET in free cell edges, demonstrating that CEACAM1-4L and CEACAM1-4S in the cell contact regions occur predominantly as microclustered assemblies.

The FRET efficiencies in free edges and cell contacts were determined for different CEACAM1 isoform combinations (Fig. 2 G). At low acceptor levels, the CEACAM1-4L/CEACAM1-4L, CEACAM1-4S/CEACAM1-4S, CEACAM1-4L/CEACAM1-4S, and CEACAM1-4ΔCyto/CEACAM1-4S combinations showed higher FRET efficiency in the cell contacts than in the free edges, which is in contrast to the ΔN–CEACAM1-3L/CEACAM1-4L and ΔN–CEACAM1-3L/CEACAM1-4S combinations that showed an opposite trend with lower FRET signals in contact regions compared with free edges. These results indicate that homophilic CEACAM1 transbinding in cell contact areas, mediated by the N-terminal domain, induces increased CEACAM1 cis-dimerization/oligomerization in the plane of the plasma membrane.

mAbs perturb the organization of CEACAM1 in the plasma membrane

Next, we investigated the effects of two different mAbs (Be9.2 and 5.4) that recognize different, nonoverlapping epitopes in the N-terminal CEACAM1 Ig domain with comparable affinities (see Materials and methods; Fig. S4). mAbs Be9.2 and 5.4 had completely opposite effects on homophilic adhesion mediated by CEACAM1-4L–YFP (Fig. 3 A), CEACAM1-4S–YFP (not depicted), or CEACAM1-4ΔCyto–YFP (not depicted). Although Be9.2 blocked adhesion, 5.4 caused a significant stimulation. The 5.4-stimulated adhesion was not caused by passive bridging between cell surface–exposed CEACAM1 and CEACAM1 on the substrate surface because the antibody did not cause attachment of cells that were treated with NSC-87877, which in itself blocked adhesion but did not decrease the surface expression of CEACAM1 as demonstrated by cytofluorimetry (Fig. S2 D). Thus, the differential effects on adhesion by the two mAbs probably reflect specific alterations of the conformation and/or supramolecular organization of the CEACAM1 ectodomains. Neither antibody had any effect on attachment to collagen I (Fig. 3 B).

To investigate whether the antibodies affected the supramolecular organization of CEACAM1, we determined the FRET efficiency in CEACAM1-4L–CFP/CEACAM1-4L–YFP-expressing cells (Fig. 4, A–E). In comparison with unstimulated cells, mAb 5.4 induced a more linear response of the FRET efficiency in free edges, which is also manifested by the slightly

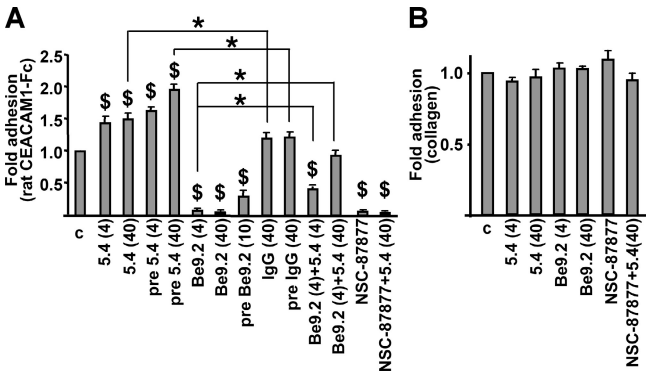

Figure 3. **Modulation of homophilic cell adhesion by mAbs.** (A and B) CEACAM1-4L–YFP-expressing cells were plated in rat CEACAM1-Fc (A)– or collagen I (B)–coated dishes for 2 h in the presence of 10% FBS with or without (c) mAb 5.4, mAb Be9.2, control IgG (concentrations in parentheses are given in microgram/milliliter), and the SHP-1/SHP-2 inhibitor NSC-87877. In some cases, CEACAM1-Fc–coated dishes were preincubated (pre) with the indicated antibodies. Attached cells were detected by crystal violet staining. The data represent mean ± SD of a representative experiment (n = 3) performed in triplicate. $, statistical significance compared with c; $, *, $P < 0.005$ (Student's t test).

increased K value (Fig. 4, A and B). This indicates that 5.4 had a dissociating effect on the CEACAM1 microclusters, thereby increasing the monomer fraction. mAb Be9.2 had an opposite effect and induced increased concentration-dependent microclustering in free edges, as manifested by a higher E_{max} value (Fig. 4 C). However, the K value remained the same as in unperturbed cells. A polyclonal anti-CEACAM1 antibody (αCC16) caused macroclustering of CEACAM1 on the cell surface (unpublished data). FRET analysis showed increased microclustering within these macroclusters with significantly lower K and higher E_{max} (Fig. 4 D). mAb Be9.2, but not 5.4, also increased the FRET efficiency in CEACAM1/CEACAM1-positive cell contact areas of confluent cells (Fig. 4 E). These results suggest that both αCC16 and Be9.2 induced a different kind of lateral association than those occurring in unperturbed cells. Support for this interpretation was obtained from size determination by sucrose gradient centrifugation (Fig. 4 F). Cells expressing CEACAM1-4L–YFP or CEACAM1-4ΔCyto–YFP were incubated with 5.4, Be9.2, or αCC16, solubilized in 1% Brij 58, and subjected to sedimentation rate centrifugation on discontinuous sucrose gradients. This demonstrated that both Be9.2 and αCC16, but not 5.4, induced formation of larger complexes of both CEACAM1-4L–YFP (not depicted) and CEACAM1-4ΔCyto–YFP (Fig. 4 F).

CEACAM1-L can bind SHP-1, SHP-2, and c-Src in a discriminatory manner

In the continued analyses, we focused on the first downstream event in the CEACAM1-L signaling process, which is binding of SHP-1/SHP-2 tyrosine phosphatases and c-Src tyrosine kinase to its tyrosine-phosphorylated cytoplasmic domain. In contrast to hematopoietic cells in which sustained tyrosine phosphorylation is achieved by homophilic binding or antibody ligation, CEACAM1-L is generally only transiently phosphorylated in epithelial cells under the influence of not well-defined growth factors (Huber et al., 1999; Chen et al., 2008). Therefore,

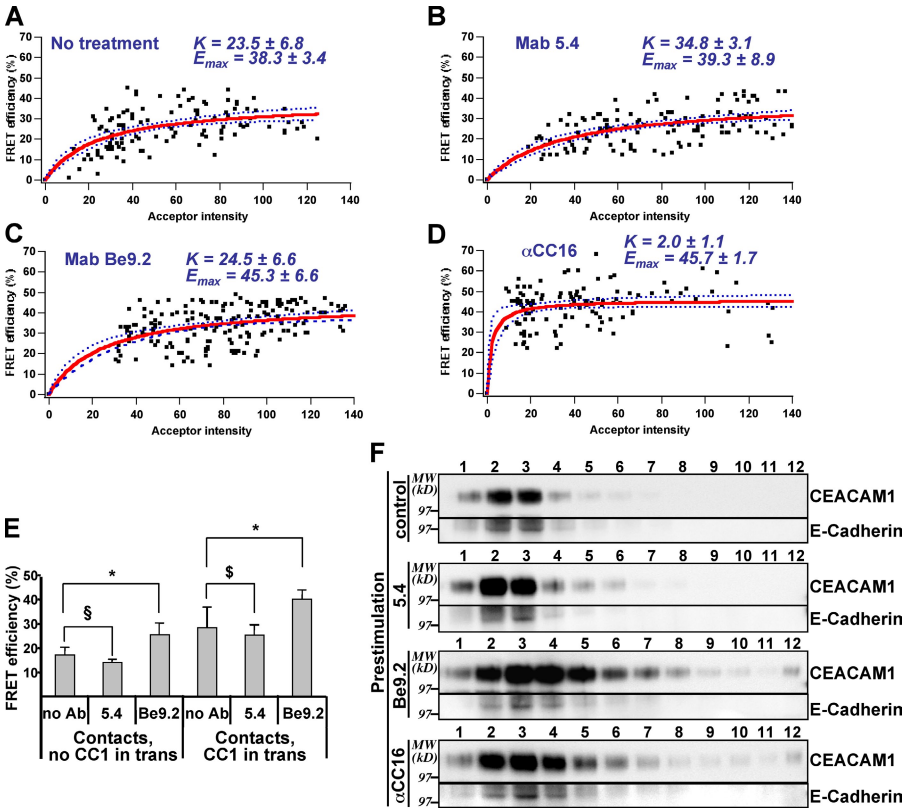

Figure 4. **Perturbation of CEACAM1 organization by anti-CEACAM1 antibodies.** (A–D) FRET for CEACAM1-4L–CFP/CEACAM1-4L–YFP-expressing cells at a 0.5–1.2 uD/A ratio. (A) Untreated cells are shown. (B–D) Incubation with mAb 5.4 (B), mAb Be9.2 (C), and pAb αCC16 (D). The least-square fits of the experimental data to Eq. 1 are shown as red curves, with 95% confidence intervals shown as flanking blue curves. The fitted values for K and E_{max} are given for each graph. (E) FRET (mean ± SD) of mixed cultures of nonexpressing and CEACAM1-4L–CFP/CEACAM1-4L–YFP-expressing cells. Contact regions between nonexpressing and CEACAM1-expressing cells (no CC1 in trans; 1.1–1.48 uD/A ratio; acceptor intensity of 17–24) and between mutually CEACAM1-expressing cells (CC1 in trans; 0.61–0.81 uD/A ratio; acceptor intensity of 34–56) were analyzed. $, P = 0.397; §, P = 0.094; *, P ≤ 0.0027 (Student's *t* test). (F) Sedimentation rate analysis of CEACAM1 after antibody treatment. Suspensions of single cells expressing CEACAM1-4ΔCyto–YFP were untreated (control) or incubated with mAb 5.4, mAb Be9.2, or pAb αCC16. Postnuclear lysates were loaded on top of a sucrose step gradient and centrifuged for 2 h at 105,000 *g*. 12 fractions (1–12; top to bottom) were collected from the top and analyzed by immunoblotting for CEACAM1 and E-cadherin. Representative blots from three different experiments are shown. Black lines indicate that intervening lanes have been spliced out. MW, molecular weight.

to induce a sustained tyrosine-phosphorylated state, we incubated the NBT-II cells with pervanadate. Pervanadate-treated, suspended cells were lysed in 1% Brij 58 and immunoprecipitated with polyclonal αCC16 or the monoclonal Be9.2 and 5.4. Although SHP-1/SHP-2/c-Src did not coprecipitate with CEACAM1-4S–YFP, all three enzymes coprecipitated with CEACAM1-4L–YFP (Fig. 5, A and B). Significant amounts of both SHP-1 and SHP-2 were coprecipitated in unstimulated cells by all three antibodies. Only a small amount of c-Src was coprecipitated by the pAb and by 5.4, whereas Be9.2 did not coprecipitate any c-Src at all. Because this indicated that the different antibodies could selectively regulate binding of the different enzymes to CEACAM1-L, we prestimulated the cells with the antibodies before solubilization. Similar to unstimulated cells, prestimulation with polyclonal αCC16 resulted in coprecipitation of all three enzymes. However, prestimulation with 5.4 increased c-Src coprecipitation and decreased coprecipitation of SHP-1, whereas coprecipitation of SHP-2 was unchanged. Prestimulation with Be9.2 caused a minor coprecipitation of c-Src but moderately increased SHP-1 coprecipitation and resulted in a more-pronounced coprecipitation of SHP-2 (Fig. 5, A and B).

Because these results indicated that the lateral supramolecular organization of CEACAM1-L might be a factor that regulates its cytoplasmic interactions, we investigated the binding abilities of CEACAM1-L monomers and dimers. Cross-linked CEACAM1-L–expressing cells were solubilized and subjected to pull-down experiments with GST–SHP-1 and GST–SHP-2. Both SHP-1 and SHP-2 bound CEACAM1-L dimers much stronger than monomers, and the preferred dimer binding was more pronounced for SHP-2 than for SHP-1 (Fig. 5 C). Pull-down experiments with c-Src did not show preferential binding of dimers (unpublished data).

Coexpression of CEACAM1-L and CEACAM1-S influences the binding of SHP-1 and SHP-2

Because CEACAM1-L and CEACAM1-S can form heterodimers (Fig. 1, D and E), we reasoned that coexpression of CEACAM1-S with a constant level of CEACAM1-L would decrease the level of the CEACAM1-L cytoplasmic domain in dimer configuration. Using antibodies recognizing the cytoplasmic domain of CEACAM1-L, we demonstrated that the expression level of CEACAM1-4L–YFP remained the same in cells that were cotransfected with CEACAM1-4S–YFP (Fig. 5 D). Immunoprecipitation of c-Src did not bring down any CEACAM1-L. However, significantly lower amounts of CEACAM1-L were coprecipitating with both SHP-1 and SHP-2 when CEACAM1-4S–YFP was coexpressed with CEACAM1-4L–YFP (Fig. 5 D). The reduction of coprecipitating CEACAM1-L was more pronounced for SHP-2 than for SHP-1, which is in agreement with the pull-down experiments that demonstrated that SHP-2 had a stronger tendency for binding CEACAM1-L dimers than SHP-1.

Recruitment of SHP-1, SHP-2, and c-Src to CEACAM1-L at the plasma membrane

To determine whether discriminatory binding occurs in intact cells, we investigated the colocalization patterns of these enzymes with CEACAM1-L in subconfluent monolayers made

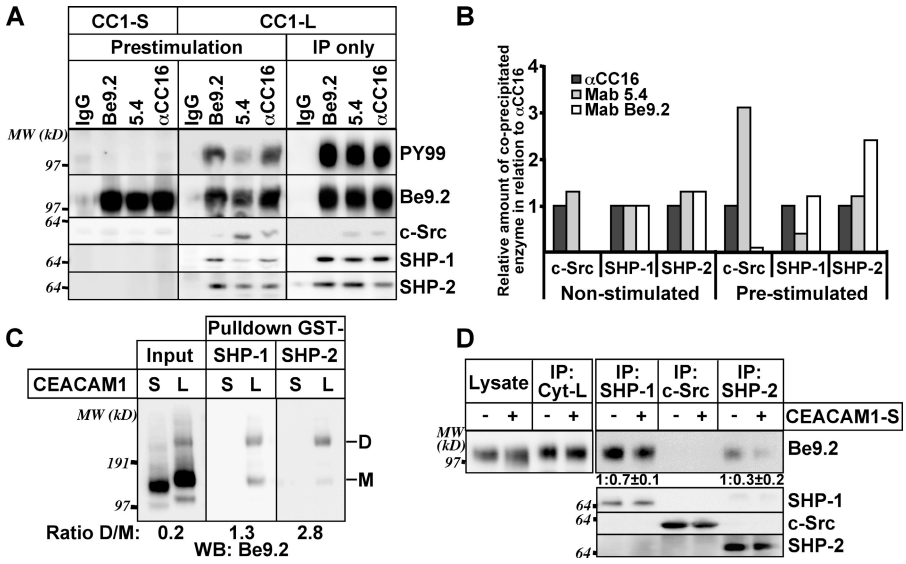

Figure 5. **Discriminatory binding of c-Src, SHP-1, and SHP-2 to CEACAM1-L.** (A) Suspensions of CEACAM1-4L–YFP or CEACAM1-4S–YFP-expressing cells were untreated or incubated with mAb 5.4, mAb Be9.2, pAb αCC16, or control IgG, treated with pervanadate, and lysed in Brij 58. Postnuclear supernatants were immunoprecipitated by antibodies coupled to protein G–Sepharose (untreated cells) or plain protein G–Sepharose (prestimulated cells). Immunoprecipitates were immunoblotted for tyrosine phosphorylation (PY99), CEACAM1 (Be9.2), or coprecipitating c-Src, SHP-1, and SHP-2. (B) Quantification of the amount of enzymes coprecipitated with CEACAM1-4L–YFP shown in A. (C) Suspensions of CEACAM1-4S–YFP- or CEACAM1-4L–YFP-expressing cells were incubated with pervanadate, cross-linked with BS^3, and lysed. SHP-1– and SHP-2–interacting proteins were affinity precipitated by GST–SHP-1 or GST–SHP-2 bound to glutathione Sepharose. Monomeric (M) and dimeric (D) CEACAM1 were detected by immunoblotting with Be9.2. Ratios of detected dimers to monomers (D/M) are shown below the blots. (D) CEACAM1-4L–YFP-expressing cells were mock transfected (−) or transiently transfected with CEACAM1-4S–YFP (+), incubated for 48 h, treated with pervanadate, and lysed. Lysates were immunoprecipitated with CEACAM1-L cytoplasmic domain–specific antibodies (Cyt-L) or with antibodies against SHP-1, SHP-2, or c-Src. CEACAM1 was detected by Be9.2, SHP-1, SHP-2, and c-Src with their respective antibodies. The ratios of CEACAM1-L precipitated in the absence and presence of coexpressed CEACAM1-S (mean ± SD of three independent experiments) are shown below the blots. IP, immunoprecipitation; WB, Western blotting; MW, molecular weight.

from mixed CEACAM1-expressing and -nonexpressing cells, which allowed simultaneous monitoring of contact zones of CEACAM1/CEACAM1-expressing (+/+), CEACAM1-expressing/nonexpressing (+/−), and CEACAM1-nonexpressing/nonexpressing (−/−) cells. Pervanadate treatment induced a strong tyrosine phosphorylation of all cell contact areas (not depicted) and resulted in a significant recruitment and colocalization of SHP-2, but not of SHP-1, in CEACAM1-4L–YFP +/+ contacts (Fig. 6, A and B). A less-pronounced recruitment of c-Src was also observed in some +/+ contacts (Fig. 6, A and B). In cells expressing ΔN–CEACAM1-3L–YFP, the recruitment of SHP-2 to +/+ contacts was reduced to <50% of that recruited to full-length CEACAM1-4L–YFP (Fig. 6 B). The recruitment patterns for c-Src did not change significantly in the ΔN–CEACAM1-3L–YFP +/+ contacts, demonstrating that c-Src recruitment to CEACAM1-L was not dependent on trans-homophilic binding by the N-terminal Ig domain (Fig. 6 B). Recruitment of SHP-2 to CEACAM1-4L–YFP +/− contacts was strongly reduced to the same levels as seen for ΔN–CEACAM1-3L–YFP +/+ and +/− contacts (Fig. 6 B), and the recruitment of c-Src to +/− contacts was reduced to the same background levels as seen in −/− contacts (Fig. 6 B).

Incubation of the cell cultures with mAbs and soluble CEACAM1-4–Fc fusion protein had no effects on SHP-1 (not depicted) but selectively affected recruitment of SHP-2 and c-Src to cell contact–localized CEACAM1-4L–YFP (Fig. 6 C). Thus, mAb 5.4 enhanced the recruitment of c-Src to both +/+ and +/− contacts. It had no significant effect on SHP-2 in +/+ contacts but significantly increased SHP-2 recruitment to +/− contacts. Adhesion-blocking mAb Be9.2 also stimulated the recruitment of c-Src to +/+ and +/− contacts, whereas it reduced recruitment of SHP-2 to +/+ and had no effect on +/− contacts. CEACAM1-4–Fc had very little effect on SHP-2 recruitment to +/+ contacts but dramatically increased SHP-2 recruitment to +/− contacts, thus mimicking trans-homophilic CEACAM1-L binding (Fig. 6 C).

To induce a more-pronounced reorganization by the mAbs and the Fc fusion protein, secondary antibodies were added for 20 min to induce macroclustering of CEACAM1-L (Fig. 7). During this short incubation time, no significant endocytic uptake of the CEACAM1 clusters occurred. CEACAM1-4–Fc clustered CEACAM1 mainly at free cell edges with little rearrangement in cell contact regions. Also, mAb 5.4 led to large cluster formation at free cell edges but left CEACAM1 in the contact regions essentially intact. mAb Be9.2 induced a pronounced macroclustering both in cell contact regions and in other locations of the cells. Upon tyrosine phosphorylation, the CEACAM1-Fc–induced CEACAM1-L macroclusters recruited SHP-2 strongly, SHP-1 weakly, and c-Src not at all (Fig. 7 B). Clustering by mAb 5.4 induced a low level recruitment of SHP-2 but had very little effect on SHP-1 or c-Src (Fig. 7 B). In contrast, clustering by mAb Be9.2 induced a pronounced recruitment of SHP-1, a low level recruitment of c-Src, and an even lower recruitment of SHP-2. (Fig. 7 B).

We next investigated whether antibody treatment induced membrane subcompartmentalization of CEACAM1 and SHP-1/SHP-2. Clustering with Be9.2, but not with 5.4 or CEACAM1-Fc (unpublished data), significantly increased the association of CEACAM1-L with detergent-insoluble membrane material independent of the tyrosine phosphorylation status (Fig. 7 C). A striking corecruitment of SHP-1 but not SHP-2 into the Be9.2-induced detergent-insoluble membrane fraction occurred after induction of tyrosine phosphorylation (Fig. 7 C).

Discussion

CEACAM1 regulates cell signaling in a cell contact–dependent manner (Scheffrahn et al., 2005; Gray-Owen and Blumberg, 2006).

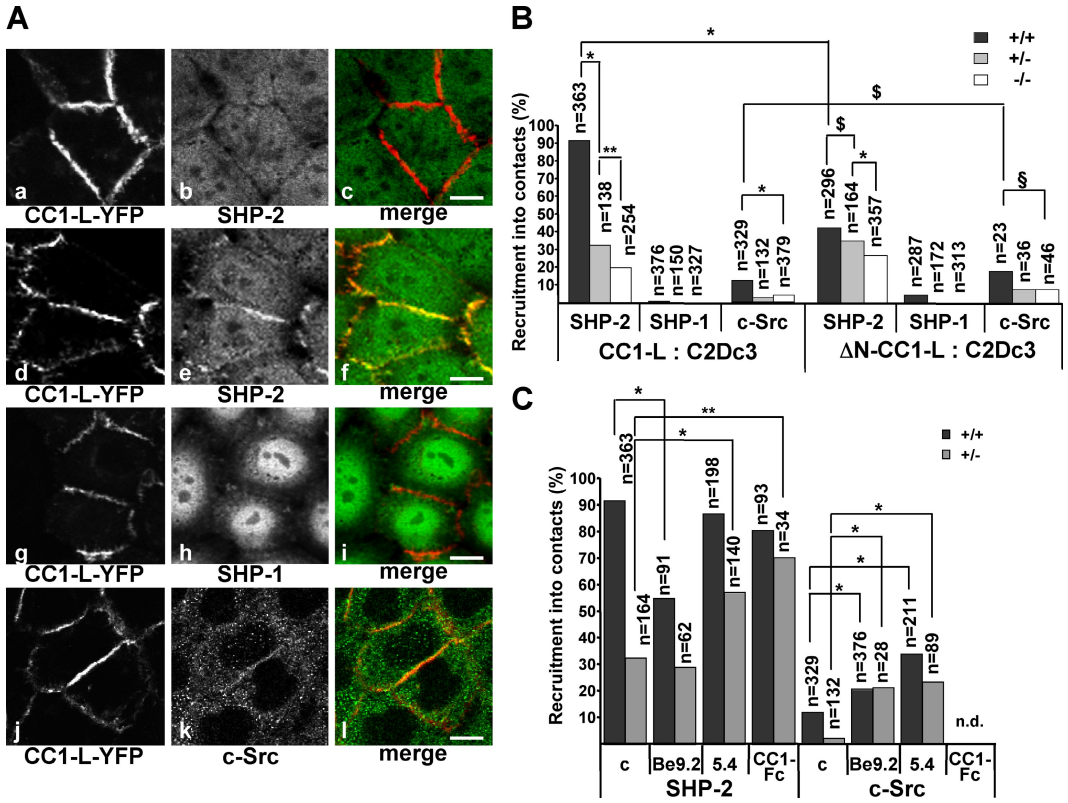

Figure 6. **CEACAM1-L–mediated recruitment of SHP-2 and c-Src.** Mixed cultures of nonexpressing and CEACAM1-4L–YFP-expressing cells or nonexpressing and ΔN–CEACAM1-3L–YFP-expressing cells were grown in monolayers; +/+, CEACAM1/CEACAM1-expressing contacts; +/−, CEACAM1-expressing/nonexpressing contacts; −/−, nonexpressing/nonexpressing contacts. (A) CEACAM1-4L–YFP was detected by YFP fluorescence; SHP-2, SHP-1, and c-Src were detected by indirect immunofluorescence (merge, false colors; red, YFP; green, Alexa Fluor 546). Nontreated cells (a–c) and pervanadate-treated cells (d–l) are shown. Bars, 10 µm. (B) Quantification of cell contact recruitment of SHP-2, SHP-1, and c-Src after pervanadate treatment (percentage of positively stained contacts). (C) Mixed cultures of nonexpressing and CEACAM1-4L–YFP-expressing cells were untreated (c) or incubated with mAb Be9.2, mAb 5.4, or CEACAM1-Fc before pervanadate treatment. Quantification was performed as described in B. (B and C) Numbers of analyzed contacts (*n*) are shown on top of each bar. Statistical significance was calculated using the two-proportion z test. *, $P \leq 0.0003$; **, $P \leq 0.001$; $, $P \leq 0.2$; §, $P \leq 0.1$.

The first downstream event in signaling by CEACAM1-L is binding and activation of SH2 domain carrying tyrosine phosphatases and kinases to its tyrosine-phosphorylated cytoplasmic domain. In this study, we have investigated the nature of the transmembrane processes that regulate these binding interactions. We show that CEACAM1-L occurs in a state of dynamic equilibrium between monomers, dimers, and oligomers and can discriminate between binding of SHP-1, SHP-2, and c-Src as a function of changes in this equilibrium. We further demonstrate that the CEACAM1-L association state equilibrium is regulated by homophilic CEACAM1 trans-binding, by expression of the smaller isoform CEACAM1-S, and by mAbs directed against the CEACAM1 N-terminal Ig domain.

Regulation of the supramolecular organization of CEACAM1

Truncation of the N-terminal D1 Ig domain of CEACAM1 showed that it mediates homophilic adhesion by reciprocal antiparallel binding, which is in agreement with previous work (Wikström et al., 1996). In addition, all CEACAM1 isoforms in the plasma membrane participated in lateral cis-binding interactions that were mediated by the ectodomain and/or the transmembrane domain. Although chemical cross-linking, coclustering, and coimmunoprecipitation showed that Ig domains D2–D4, and maybe the transmembrane domain, participate in cis-binding, FRET determinations demonstrated that Ig domain D1 also exhibits a strong, mutual cis-interaction. Furthermore, the FRET experiments revealed that antiparallel D1-mediated trans-homophilic binding between CEACAM1 molecules in cell junctions triggered increased cis-interactions between these molecules, which agrees with our recent findings in proteoliposomes (Klaile et al., 2009). Thus, both the liposome experiments and the present data indicate that the N-terminal Ig domain transmits allostery that is important for adhesion-triggered rearrangements of the lateral organization of CEACAM1.

CEACAM1 does not occur either as monomers, dimers, or oligomers in different parts of the plasma membrane but as a mixture of these species. The relative proportions of CEACAM1 monomers, dimers, and oligomers are regulated by the expression level and by trans-homophilic binding in cell junctions. In addition, the expression ratio of the cytoplasmic domain isoforms CEACAM1-L and CEACAM1-S is an important regulator of the monomer/dimer state of the cytoplasmic domain of CEACAM1-L because CEACAM1-L and CEACAM1-S form heterodimers.

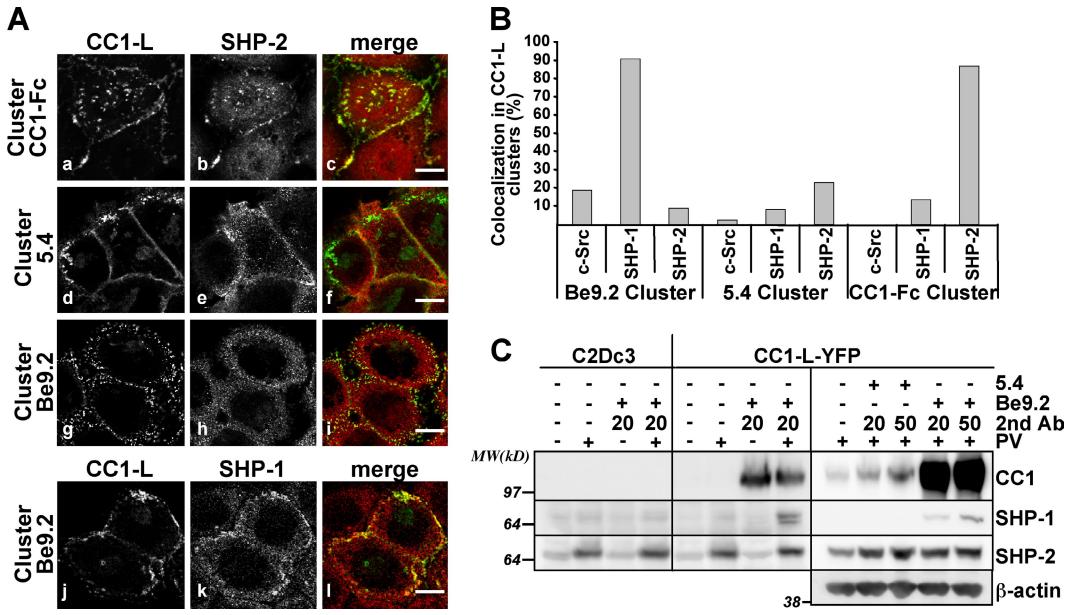

Figure 7. **Superclustering of CEACAM1 and recruitment of c-Src, SHP-1, and SHP-2.** (A) CEACAM1-4L–YFP-expressing cells were incubated with rat CEACAM1-Fc, mAb 5.4, or mAb Be9.2 followed by anti–human Fc IgG or anti–mouse IgG. The cellular localization of CEACAM1-4L–YFP (a, d, g, and j), SHP-1 (k), and SHP-2 (b, e, and h) was analyzed by confocal microscopy. Merged images (c, f, i, and l) demonstrate colocalization of SHP-2 with CEACAM1-Fc–induced clusters and SHP-1 with Be9.2-induced clusters (red, SHP-1/SHP-2; green, false-color YFP). Bars, 10 µm. (B) Quantification of c-Src, SHP-1, and SHP-2 colocalized with CEACAM1-4L–YFP clusters. (C) Immunoblots of detergent-insoluble material after clustering of CEACAM1-L–YFP. C2Dc3- or CEACAM1-L–YFP-expressing cells were untreated (−) or preincubated (+) with primary antibodies for 20 min and secondary antibodies for 20 or 50 min. Pervanadate (PV) was added (+) during the last 5 min. The cells were lysed in ice-cold 1% Triton X-100/HBSM, and the insoluble material was analyzed for CEACAM1, SHP-1, SHP-2, and β-actin. MW, molecular weight.

These findings do not completely agree with our previous model in which we suggested that trans-homophilic adhesion is mediated by monomeric CEACAM1 and that cis-dimeric CEACAM1 occurs on surfaces that are not engaged in cell–cell adhesion (Öbrink et al., 2002). This model was based on the limited biochemical/cell biological data that were available at that time, and one of the aims of this study was to produce experimental data that would show the role of CEACAM1 monomers and cis-dimers in cell adhesion. Together with the accompanying paper (Klaile at al., 2009), we can now demonstrate that adhesion is mediated both by monomeric and cis-dimeric CEACAM1 and that trans-homophilic binding triggers increased cis-dimerization. One prediction of the previous model, which we now demonstrate to be true, was that coexpression of CEACAM1-S and CEACAM1-L would decrease the extent of CEACAM1-L cis-homodimerization caused by formation of CEACAM1-L/CEACAM1-S cis-heterodimers. Another prediction, based on molecular modeling, was that monomeric CEACAM1-L would favor SHP-1/SHP-2 binding, whereas dimeric CEACAM1-L would favor c-Src binding. However, the experimental data demonstrate that the tyrosine phosphatases prefer dimeric CEACAM1-L, whereas c-Src does not show any particular preference for dimeric over monomeric CEACAM1-L. SHP-1/SHP-2 has two SH2 domains, both of which can bind to either of the two phosphotyrosine-based binding sequences in the cytoplasmic domain of CEACAM1-L (Sigmundsson, 2004). The preference of the phosphatases for dimeric CEACAM1-L might thus be caused by simultaneous binding to two CEACAM1-L molecules, which was suggested previously (Öbrink and Hunter, 1998).

Discriminatory binding of SHP-1, SHP-2, and c-Src is determined by the supramolecular organization of CEACAM1-L

One of the important findings in the present investigation was that CEACAM1-L could discriminate between binding of c-Src, SHP-1, and SHP-2 in a manner that was regulated and dependent on its supramolecular organization. The discriminatory binding of the three enzymes might be the basis for the different signal regulatory effects by CEACAM1, which have been found to be both inhibitory and stimulatory (Greicius et al., 2003; Scheffrahn et al., 2005; Gray-Owen and Blumberg, 2006; Slevogt et al., 2008). The relative binding proportions of the enzymes depended on the state of lateral associations of CEACAM1-L and were controlled by CEACAM1 trans-homophilic binding in cell junctions. As outlined in the model in Fig. 8, the allosterically induced microclustering of CEACAM1 will bring the cytoplasmic domains of CEACAM1-L molecules in close proximity, which will lead to intensified interactions with cytoplasmic phosphatases upon tyrosine phosphorylation and to subsequent changes of the ratio of bound SHP-1/SHP-2 and c-Src. In general, SHP-2 was the predominant binding partner for CEACAM1-L in NBT-II cells in which it was recruited to essentially all CEACAM1-L–containing cell junctions upon induction of tyrosine phosphorylation. This is in contrast to hematopoietic cells in which SHP-1 seems to be the primary binding and signaling partner (Singer et al., 2005; Nagaishi et al., 2006). The preferred binding of SHP-2 over SHP-1 may partly result from the higher affinity of SHP-2 for dimeric CEACAM1-L but may most likely be the result of different compartmentalization of the two phosphatases. SHP-1 and SHP-2 differ in their

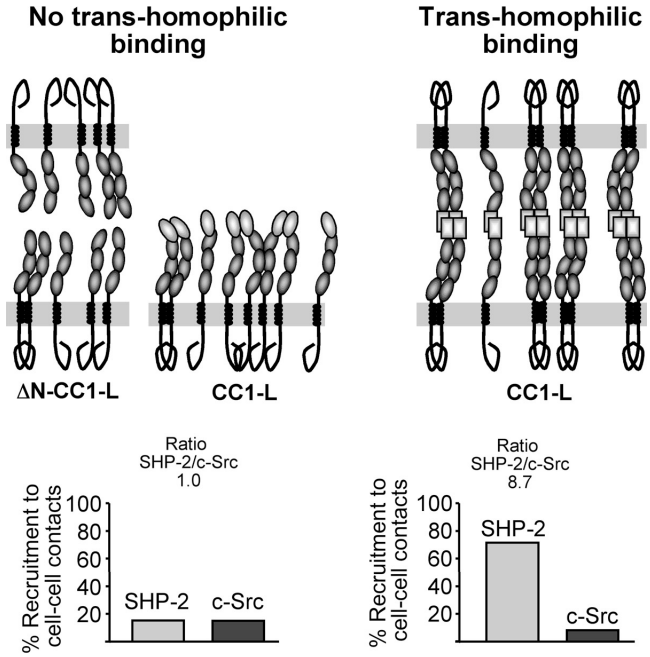

Figure 8. **A model for transmembrane signaling by CEACAM1-L.** Trans-homophilic binding mediated by the N-terminal Ig domain induces cis-dimerization of CEACAM1 by an allosteric mechanism. Cis-homodimerization of CEACAM1-L brings its cytoplasmic domains together, which interact to change the relative binding affinities for SHP-2 and c-Src. Therefore, increased CEACAM1-L homodimerization results in increased binding/activation of SHP-2 but no change or a slightly reduced binding/activation of c-Src. The displayed recruitment data for SHP-2 and c-Src are calculated from the data presented in Fig. 6 B.

C-terminal amino acid sequences (Poole and Jones, 2005), and SHP-1 has a bipartite nuclear localization (Craggs and Kellie, 2001) motif and a short sequence responsible for targeting to lipid rafts (Sankarshanan et al., 2007), both of which are missing in SHP-2. Thus, SHP-1 may not be available for binding to dimeric CEACAM1-L in cell junctions.

Because the monomer/dimer/oligomer balance can be regulated by the cell, it seems likely that CEACAM1 does not operate as an on/off switch but rather regulates cell signaling in a context-dependent, continuous manner. Because both of the total expression level and the CEACAM1-S/CEACAM1-L expression ratios vary considerably between various cell types, between different functional states of the same cell type, during different phases of the cell cycle, and between normal and cancer cells (Singer et al., 2000, 2002; Gaur et al., 2008), it confers on CEACAM1 a broad potential in regulating a variety of outside-in signaling events. In addition, we found that the extracellular recognition activities of CEACAM1 itself can be controlled by unidentified factors in FBS and by intracellular tyrosine kinase/phosphatase-regulated reactions. Because the cytoplasmic tail of CEACAM1 was dispensable in this context, it is unlikely that phosphorylation/dephosphorylation events within this domain regulate the affinity of the extracellular domain in an inside-out signaling process. Rather, it implicates cytoplasmic events downstream of cytokine/growth factor receptor activation, which either involve cytoskeletal rearrangements or modifications of a hitherto unidentified lateral binding partner of CEACAM1. Thus, it is obvious that CEACAM1 participates in a complex network of cellular control mechanisms.

The supramolecular organization and cytoplasmic interactions of CEACAM1 can be perturbed by antibodies

Two mAbs directed against different epitopes in the N-terminal Ig domain had opposite effects both on CEACAM1-mediated homophilic adhesion and on lateral CEACAM1 interactions in the plasma membrane. The differential effects suggest that the two mAbs stabilize different conformations, which is in agreement with the allosteric regulation of the homophilic binding activities of the N-terminal Ig domain. Ligation with mAb 5.4 increased the trans-homophilic adhesion and at the same time led to a reduction of CEACAM1 microclustering. In contrast, mAb Be9.2 inhibited trans-binding but induced a higher level of microclustering. The blocking effect of mAb Be9.2 was partly overcome by simultaneous ligation with mAb 5.4, indicating that the epitope-mediating trans-adhesion was not simply shielded by Be9.2. mAb Be9.2 therefore seems to induce a conformation of the N domain that is no longer suitable for trans-homophilic binding. In addition, the two antibodies affected the interactions with c-Src, SHP-1, and SHP-2 in strikingly different ways. However, the antibody effects were different in intact and solubilized cells. The coprecipitation patterns in solubilized cells, which reflect the average interactions of all CEACAM1-L, indicate which types and levels of interactions that can occur. The recruitment patterns observed in intact cells show which types of interactions that do occur with CEACAM1-L organized in cell junctions, which is different from what can occur, presumably because of different compartmentalization of the enzymes. Cross-linking of the primary mAbs with secondary antibodies induced a pronounced rearrangement of CEACAM1-L on the cell surface and a dramatic change in the recruitment of SHP-1/SHP-2/c-Src (Fig. 7). The almost-exclusive recruitment of SHP-1 to CEACAM1-L super clustered by mAb Be9.2 might be explained by colocalization of the two molecules in lipid rafts because superclustering with mAb Be9.2 but not with mAb 5.4 caused association of CEACAM1-L with detergent-resistant membrane domains. The activating mechanism for recruitment of SHP-1 remains elusive at present, but it has been shown that serine phosphorylation of its C terminal can regulate the cytoplasmic/nuclear/raft localization (Liu et al., 2007). The almost exclusive recruitment of SHP-2 to CEACAM1-L super clustered by CEACAM1-Fc was most likely caused by mimicking of CEACAM1-L trans-homophilic binding. The different effects of the mAbs make CEACAM1 a potentially interesting but also challenging target for mAb-based therapy of human disease.

Materials and methods

Reagents and antibodies

All reagents were obtained from Sigma-Aldrich or Merck if not stated otherwise. Anti–rat CEACAM1 mouse monoclonal (Be9.2 and 5.4) and rabbit polyclonal (αCC16 and anti–CEACAM1-L–Cyto [αcyto]) antibodies were described previously (Becker et al., 1986; Singer et al., 2000; Budt et al., 2002). All antibodies recognized monomeric and dimeric CEACAM1-L equally well (Fig. S3). The mAbs Be9.2 and 5.4 recognized different, non-overlapping epitopes in the N-terminal Ig domain of rat CEACAM1 as

determined by BIAcore-binding analysis but had similar binding affinity toward cell surface–expressed CEACAM1 (Fig. S4). Other mouse mAbs used were anti-CD56 (T199; Dako), anti-Src (B-12; Santa Cruz Biotechnology, Inc.), anti–α3-integrin (clone 42; BD), anti–E-cadherin (clone 34; BD), anti–α6-integrin (4E9G8; DPC Biermann), and anti-GFP (clones 7.1 and 13.1; Roche). The following primary pAbs were used: rabbit anti-SHP-1 (C-19), rabbit anti–SHP-2 (C-18), rabbit anti-Src (N-16), rabbit anti–cyclin D1 (C-20; Santa Cruz Biotechnology, Inc.), and rabbit antiactin (20–33; Sigma-Aldrich). The following secondary antibodies were used: goat anti–mouse IgG Alexa Fluor 546 and 488 conjugates, goat anti–rabbit IgG Al exa Fluor 633, 546, and 488 conjugates (Invitrogen), unconjugated and peroxidase-conjugated goat anti–mouse, and goat anti–rabbit IgG (Jackson ImmunoResearch Laboratories, Inc.).

Cell culture, cloning, and expression procedures

Culture reagents were obtained from Invitrogen. Rat bladder carcinoma-derived epithelial NBT-II cells (Toyoshima et al., 1971) were grown at 37°C in 5% CO_2 in high glucose DME/10% FBS/penicillin/streptomycin and 500 µg/ml G418 and/or 10–40 µg/ml Blasticidin S if indicated. Transfections were performed using Lipofectamine 2000 (Invitrogen), and cloning was performed by limited dilution. Correct sequences and reading frames of all constructs were verified by sequencing.

Rat CEACAM1 shRNA vector. Rat CEACAM1 shRNA targeting nucleotides 1,446–1,464 in rat CEACAM1 (annealed 5′-GGTGGATGACGTCTCATACTTCAAGAGAGTATGAGACGTCATCCACCTTTTTT-3′ and 5′-AATTAAAAAAGGTGGATGACGTCTCATACTCTCTTGAAGTATGAGACGTCATCCACCGGCC-3′; Edlund et al., 1993) was expressed under the U6 promoter of pSilencer (Applied Biosystems) in pEGFP-N1 (the EGFP cassette was removed; Takara Bio Inc.).

Recombinant transmembrane rat CEACAM1. Rat CEACAM1-4L and CEACAM1-4S cDNAs (Olsson et al., 1995) were inserted into the XbaI–HindIII sites of pcDNA3(+) (Invitrogen). The cDNAs of monomeric CFP and YFP (Kim et al., 2003) were provided by T. Springer (Harvard Medical School, Boston, MA), amplified by PCR (Phusion polymerase; Finnzyme; 5′-CCTGATCCAACACAAGGAAATTCTGGCCTCTCAGGAGGTGGCATGGTGAGCAAGGGC-3′ and 5′-AGATCCAATCACAATGCCTGCAATGGCACCCTCTGATCCTCCTCCCTTGTACAGCTCGTC-3′), and were inserted by homologous recombination into the extracellular domain between membrane proximal serine (S422) and glutamic acid (E423) residues (-G-L-S-CFP/YFP-E-G-A-; Edlund et al., 1993) flanked by 3-Gly linkers. Silent mutations in the CEACAM1 sequence used for the shRNA were introduced by amplification of the plasmid (5′-GTGAGCTATTCTGTCCTGAACTTCAATGC-3′ and 5′-ATCGTCGACCTTGTTAGGAGAGTCGT-3′) and self-ligation. To obtain vectors with Blasticidin resistance, the XbaI–HindIII cassettes of CEACAM1-CFP/YFP constructs were ligated into pcDNA6/V5a (Invitrogen). To obtain CEACAM1-4ΔCyto–YFP, pcDNA6/CEACAM1-4L–YFP was amplified and self-ligated using the primers 5′-TAGAAGAAGTGACATTGTCTGTCCTG-3′ and 5′-ATAAAGGAAGTATGCCAGCGCT-3′ to introduce a stop codon terminating the polypeptide chain at Y448. To obtain ΔN–CEACAM1-3L–YFP, pcDNA6/CEACAM1-4L–YFP was amplified and self-ligated using the primers 5′-GGTGACTTGGGCAGTGGT-3′ and 5′-GCATTACAAAAGCCCAACGTC-3′ (omitting the D1 domain).

Soluble CEACAM1 ectodomains. For the rat and human D(1–4)-Fc constructs, rat and human CEACAM1 ectodomains (GenBank accession no. J04963 and X16354) and human IgG Fc (GenBank accession no. BC014258) were amplified (rat CEACAM1, 5′-AAGCTTTAGCAGGCAGCAGAGACTATGG-3′ and 5′-GAATTCAGAATTTCCTTGTGTTGGATCAGG-3′; human CEACAM1, 5′-AAGCTTACCATGGGGCACCTCTCAGCC-3′ and 5′-GAATTCAGGTGAGAGGCCATTTTCTTG-3′; and human Fc, 5′-GAATTCATGGCACCTGAACTCCTGGGGGGACC-3′ and 5′-CTCGAGTCATTTACCCGGAGACAGGGAGAGGC-3′) and ligated sequentially into the HindIII–EcoRI–XhoI sites of pcDNA3.1(+) (Invitrogen). To obtain the rat D(2–4)-Fc construct, the vector containing rat D(1–4)-Fc was amplified (5′-GGTGACTTGGGCAGTGGT-3′ and 5′-GCATTACAAAAGCCCAACGTC-3′; omitting the D1 domain) and self-ligated. Plasmids were transfected into HEK293 cells, and proteins were allowed to accumulate in serum-free Pro293s-CDM medium (BioWhittaker). Fc fusion proteins were purified by protein A–Sepharose affinity chromatography (HiTrap Protein A HP; GE Healthcare).

Recombinant phosphatases. GST-tagged catalytically inactive mouse SHP-1 (C>S) and SHP-2 in pGEX-2TK were provided by N. Beauchemin (McGill University, Montreal, Quebec, Canada). Recombinant proteins were expressed in *Escherichia coli* BL21 (DE3)pLysS and purified by affinity chromatography on glutathione Sepharose 4 Fast Flow (GE Healthcare).

Cell adhesion

Cell adhesion measurements were performed as described previously (Müller et al., 2005). In brief, 96-well plates (Maxisorb immuno plate; Thermo Fisher Scientific) were coated with 50 µl rat D(1–4)-Fc (80 µg/ml), rat D(2–4)-Fc (80 µg/ml), human D(1–4)-Fc (80 µg/ml), BSA (10 mg/ml), or rat tail collagen I (20 µg/ml) overnight at 4°C blocked with 1% BSA/PBS for 1 h at 37°C and washed with PBS. Cells were grown to 70% confluency and trypsinized; trypsin was inhibited with soybean trypsin inhibitor (Roche). For analyzing the effect of serum, the cells were serum starved 1 h before trypsination. 3×10^4 cells per well were seeded in the absence or presence of the following inhibitors and antibodies: 10 µM PP2, 100 µM NSC-87877, 4–40 µg/ml mAbs 5.4 and Be9.2, and isotype control IgG (anti-huCD56). In the analyses of the SHP inhibitor NSC-87877, the cells were cultured in 50 µg/ml NSC-87877 for 2 d before adhesion determination. Cells were allowed to attach for 2 h (at 37°C in 5% CO_2), and nonattached cells were removed by washing. Attached cells were fixed (4% PFA/PBS) and stained with 0.1% crystal violet, bound crystal violet was extracted with 0.5% Triton X-100/H_2O, and the OD was determined at 595 nm.

Immunoprecipitation and immunoblotting

Immunoprecipitation. Trypsinized, suspended cells in serum-free medium were incubated with or without 40 µg/ml antibodies for 10 min followed by 0.1 mM pervanadate for 5 min at 37°C and collected by centrifugation. Adherent cells were incubated with 0.1 mM pervanadate for 5 min at 37°C and scraped into lysis buffer. Pelleted and scraped cells were lysed immediately with ice-cold HBSM (25 mM Hepes, 150 mM NaCl, and 2 mM $MgCl_2$, pH 7.2)/1% Brij 58 supplemented with protease (Sigma-Aldrich) and phosphatase inhibitor cocktails (PhosStop; Roche), 1 mM PMSF, and 0.1 mM pervanadate. After 1 h on ice, the lysates were cleared by centrifugation at 15,000 *g*, and equal amounts of protein, determined by the BCA method (Thermo Fisher Scientific), were immunoprecipitated by protein A–Sepharose or protein G–Sepharose beads plain or precoupled with 2–3 µg antibodies for 2–3 h at 4°C. After washing (three times in HBSM/0.1% Brij 58), the beads were boiled in Laemmli sample buffer and subjected to SDS-PAGE and immunoblotting.

Analysis of detergent-insoluble membranes. Cells were incubated with 10 µg/ml primary antibodies (at 37°C for 20 min) and 10 µg/ml secondary antibodies (at 37°C for 20 or 50 min) and lysed with ice-cold 1% Triton X-100/HBSM for 1 h. Insoluble material was pelleted by centrifugation at 17,000 *g* for 10 min. Pellets were washed with HBSM and boiled in 2× Laemmli buffer. After digestion of DNA with Benzonase (Sigma-Aldrich), equal volumes were analyzed by immunoblotting.

Immunoblotting. Electrophoretically separated components were transferred to nitrocellulose filters (Schleicher & Schüll). HRP-conjugated secondary antibodies were detected by ECL (SuperSignal West Pico Chemiluminescent Substrate; Thermo Fisher Scientific) using a digital system (LAS-1000; Fujifilm) or films (BioMax MS; Kodak). Quantification was performed in the Image Gauge software (Fujifilm) or on films scanned and analyzed with the ImageJ software (National Institutes of Health). Images were imported into Photoshop (Adobe) for processing.

Chemical cross-linking and pull-down

Adherent or trypsinized cells were washed with serum-containing medium and PBS supplemented with 1 mM $CaCl_2$/2 mM $MgCl_2$ (PBS/Mg/Ca) at RT. Cross-linking was initiated by addition of 0.5 mg/ml bis-sulfosuccinimidyl suberate (BS^3) freshly prepared in PBS/Mg/Ca. After 15 min, the reaction was quenched with 50 mM Tris/HCl in PBS, pH 7.9, and the cells were lysed for 1 h in 2% Triton X-100/0.2% SDS/HBSM supplemented with protease/phosphatase inhibitor cocktails, 1 mM PMSF, and 0.1 mM pervanadate. The lysates were cleared by centrifugation at 15,000 *g* and analyzed for CEACAM1 by SDS-PAGE/immunoblotting. For GST pull-down experiments, cells were washed and incubated with 0.1 mM pervanadate in PBS (for 5 min at 37°C), pelleted, resuspended in PBS/BS^3, cross-linked, and lysed in 2% Triton X-100/0.2% SDS/HBSM. Cleared lysates were diluted 1:2 with HBSM, and equal volumes were incubated with 4 µg GST-tagged SHP-1 or SHP-2 (precoupled to glutathione Sepharose) for 3 h at 4°C. The beads were washed three times with 0.1% Triton X-100/HBSM and boiled in Laemmli SDS sample buffer. Affinity-purified proteins were analyzed and detected by immunoblotting.

Sedimentation analysis

Subconfluent NBT-II cells expressing CEACAM1-4L–YFP or CEACAM1-4ΔCyto–YFP were trypsinized and incubated in serum-free medium with or without 40 µg/ml antibodies for 10 min at 37°C. The cells were pelleted and

lysed in 1% Brij 58/HBSM supplemented with protease inhibitor cocktail and 1 mM PMSF for 1 h at 4°C. The lysates were centrifuged at 15,000 *g*, 200 µl supernatants was loaded on top of discontinuous gradients made from 1 ml each of 48, 35, 25, 17, 10, and 3% (wt/wt) sucrose/HBSM, and were centrifuged at 100,000 *g* for 120 min in an ultracentrifuge rotor (70.1 Ti; Beckman Coulter). 516 µl fractions was collected from the top, and equal volumes were analyzed by SDS-PAGE/immunoblotting.

Immunofluorescence and confocal microscopy

For colocalization experiments, cells were seeded sparsely on coverslips and grown for 2 d to 70% confluence. After serum starvation (1 h), antibodies (20 µg/ml) were added for 30 min at 37°C or in clustering experiments for 20 min plus 20-min secondary antibodies (10 µg/ml). The cells were incubated with 0.1 mM pervanadate (for 5 min at 37°C), fixed in 4% PFA/PBS (10 min), permeabilized in 4% PFA/PBS/0.025% saponin (10 min), blocked with 1% BSA/PBS (1 h), and incubated with primary antibodies (5 µg/ml) for 2 h or overnight and with appropriate secondary antibodies (1:200) for 2 h. For coclustering of CEACAM1 isoforms, cells were seeded sparsely in the presence of 20 µg/ml primary anti-CEACAM1 antibodies (for 1 h at 37°C) on poly-L-lysine–coated coverslips, and incubated with secondary antibodies for 20 min at 37°C before fixation. The coverslips were mounted in Vectashield (Vector Laboratories) and sealed with nail polish. Confocal images were recorded in a laser-scanning confocal inverse microscope (Axiovert 200; Carl Zeiss, Inc.) equipped with argon, HeNe1, and HeNe2 lasers and a detector system (LSM 510 META; Carl Zeiss, Inc.) with a 63× NA 1.4 Plan Apochromat (Carl Zeiss, Inc.) or a 40× NA 0.75 Plan Neofluar objective (Carl Zeiss, Inc.). Images were imported from the LSM 5 Image Examiner software (version 3.2; Carl Zeiss, Inc.) into Photoshop (Adobe) for processing.

FRET

Cells stably transfected with one CFP/YFP-tagged donor/acceptor CEACAM1 isoform were transiently transfected with a complementary CFP/YFP-tagged donor/acceptor isoform, and FRET was measured by acceptor photobleaching of fixed cells 24–48 h after the transient transfection. Both cultured, adherent cells and trypsinized cells that were plated for 90 min in serum-containing medium on coverslips coated with 0.002% poly-L-lysine or Matrigel (1:100 in PBS) were examined. The attached cells were incubated with or without 20 µg/ml antibodies for 20 min at 37°C, fixed with 4% PFA/PBS for 10 min at RT, and mounted in Vectashield. Fields containing one to four cells were chosen, and prebleach images of CFP and YFP were collected separately with a 40× NA 0.75 oil immersion objective. CFP was excited at 458 nm with 35.1% laser intensity emission and detected at 475–500 nm with detector gain of 955; YFP was excited at 514 nm with 3% laser intensity and detected at 530–560 nm with detector gain of 610. A selected region of interest (ROI) was photobleached with the 514-nm laser line (100% intensity; 100–140 iterations), and postbleach CFP and YFP images were collected. After image registration and background subtraction, the fluorescent signal outlining the cell membrane was divided into 5–15 ROIs per cell that were each analyzed independently in the ImageJ or the LSM 510 software (Carl Zeiss, Inc.). Selected ROIs exhibiting saturation in either the donor or acceptor channel were eliminated from further analysis. For FRET analysis of cell contact regions, contacting cells with similar intensity levels of CFP and YFP were chosen, and the relative intensities for each fluorophor were divided by two to obtain fluorescence signals originating from one plasma membrane only. FRET efficiency (E) was calculated as $E\ (\%) = 100 \times [1 - (F_{CFPpre}/F_{CFPpost})]$, where F_{CFPpre} and $F_{CFPpost}$ are the mean CFP emission intensities before and after YFP photobleaching, respectively. Data were fitted to Eq. 1 (see Results) by a least-squares procedure using IGOR Pro (version 6.0; WaveMetrics, Inc.).

Online supplemental material

Fig. S1 shows CEACAM1 knockdown in C2Dc3 cells by stable transfection with shRNA and analysis of reexpressed, YFP-tagged CEACAM1 isoforms by immunoblotting, confocal microscopy, and chemical cross-linking. Fig. S2 shows the ability of CEACAM1-YFP isoforms expressed in NBT-II cells to mediate homophilic adhesion, the effect of kinase and phosphatase inhibitors on adhesion, and the effect of inhibitors and anti-CEACAM1 antibodies on surface expression levels of CEACAM1. Fig. S3 shows the recognition of monomeric and dimeric CEACAM1 by various anti-CEACAM1 antibodies. Fig. S4 shows the binding of mAbs Be9.2 and 5.4 to cell surface–exposed CEACAM1 by flow cytometry. Online supplemental material is available at http://www.jcb.org/cgi/content/full/jcb.200904150/DC1.

We are grateful to Dr. T. Springer for providing plasmids containing monomeric CFP and YFP, Dr. L. Lucka (Charité-Universitätsmedizin Berlin, Berlin, Germany) for providing anti–CEACAM1-L–cyto serum, and Dr. N. Beauchemin for providing plasmids with GST-tagged SHP-1 and SHP-2.

This work was supported by the Swedish Research Council (project No. 05200), the Swedish Cancer Foundation (project No. 07 0629), Marianne and Markus Wallenbergs Stiftelse, and the Karolinska Institutet.

Submitted: 28 April 2009
Accepted: 20 October 2009

References

Beauchemin, N., P. Draber, G. Dveksler, P. Gold, S. Gray-Owen, F. Grunert, S. Hammarström, K.V. Holmes, A. Karlsson, M. Kuroki, et al. 1999. Redefined nomenclature for members of the carcinoembryonic antigen family. *Exp. Cell Res.* 252:243–249. doi:10.1006/excr.1999.4610

Becker, A., R. Neumeier, C. Heidrich, N. Loch, S. Hartel, and W. Reutter. 1986. Cell surface glycoproteins of hepatocytes and hepatoma cells identified by monoclonal antibodies. *Biol. Chem. Hoppe Seyler.* 367:681–688.

Boulton, I.C., and S.D. Gray-Owen. 2002. Neisserial binding to CEACAM1 arrests the activation and proliferation of CD4+ T lymphocytes. *Nat. Immunol.* 3:229–236. doi:10.1038/ni769

Brümmer, J., M. Neumaier, C. Göpfert, and C. Wagener. 1995. Association of pp60c-src with biliary glycoprotein (CD66a), an adhesion molecule of the carcinoembryonic antigen family downregulated in colorectal carcinomas. *Oncogene.* 11:1649–1655.

Budt, M., I. Cichocka, W. Reutter, and L. Lucka. 2002. Clustering-induced signaling of CEACAM1 in PC12 cells. *Biol. Chem.* 383:803–812. doi:10.1515/BC.2002.084

Chen, Z., L. Chen, S.W. Qiao, T. Nagaishi, and R.S. Blumberg. 2008. Carcinoembryonic antigen-related cell adhesion molecule 1 inhibits proximal TCR signaling by targeting ZAP-70. *J. Immunol.* 180:6085–6093.

Craggs, G., and S. Kellie. 2001. A functional nuclear localization sequence in the C-terminal domain of SHP-1. *J. Biol. Chem.* 276:23719–23725. doi:10.1074/jbc.M102846200

Ebrahimnejad, A., T. Streichert, P. Nollau, A.K. Horst, C. Wagener, A.-M. Bamberger, and J. Brümmer. 2004. CEACAM1 enhances invasion and migration of melanocytic and melanoma cells. *Am. J. Pathol.* 165:1781–1787.

Edlund, M., H. Gaardsvoll, E. Bock, and B. Öbrink. 1993. Different isoforms and stock-specific variants of the cell adhesion molecule C-CAM (cell-CAM 105) in rat liver. *Eur. J. Biochem.* 213:1109–1116. doi:10.1111/j.1432-1033.1993.tb17860.x

Gaur, S., J.E. Shively, Y. Yen, and R.K. Gaur. 2008. Altered splicing of CEACAM1 in breast cancer: identification of regulatory sequences that control splicing of CEACAM1 into long or short cytoplasmic domain isoforms. *Mol. Cancer.* 7:46. doi:10.1186/1476-4598-7-46

Gray-Owen, S.D., and R.S. Blumberg. 2006. CEACAM1: contact-dependent control of immunity. *Nat. Rev. Immunol.* 6:433–446. doi:10.1038/nri1864

Greicius, G., E. Severinson, N. Beauchemin, B. Öbrink, and B.B. Singer. 2003. CEACAM1 is a potent regulator of B cell receptor complex-induced activation. *J. Leukoc. Biol.* 74:126–134. doi:10.1189/jlb.1202594

Gu, A., W. Tsark, K.V. Holmes, and J.E. Shively. 2009. Role of *Ceacam1* in VEGF induced vasculogenesis of murine embryonic stem cell-derived embryoid bodies in 3D culture. *Exp. Cell Res.* 315:1668–1682. doi:10.1016/j.yexcr.2009.02.026

Horst, A.K., W.D. Ito, J. Dabelstein, U. Schumacher, H. Sander, C. Turbide, J. Brümmer, T. Meinertz, N. Beauchemin, and C. Wagener. 2006. Carcinoembryonic antigen-related cell adhesion molecule 1 modulates vascular remodeling in vitro and in vivo. *J. Clin. Invest.* 116:1596–1605. doi:10.1172/JCI24340

Huber, M., L. Izzi, P. Grondin, C. Houde, T. Kunath, A. Veillette, and N. Beauchemin. 1999. The carboxy-terminal region of biliary glycoprotein controls its tyrosine phosphorylation and association with protein-tyrosine phosphatases SHP-1 and SHP-2 in epithelial cells. *J. Biol. Chem.* 274:335–344. doi:10.1074/jbc.274.1.335

Hunter, I., H. Sawa, M. Edlund, and B. Öbrink. 1996. Evidence for regulated dimerization of cell-cell adhesion molecule (C-CAM) in epithelial cells. *Biochem. J.* 320:847–853.

Kenworthy, A.K., and M. Edidin. 1998. Distribution of a glycosylphosphatidylinositol-anchored protein at the apical surface of MDCK cells examined at a resolution of <100 A using imaging fluorescence resonance energy transfer. *J. Cell Biol.* 142:69–84. doi:10.1083/jcb.142.1.69

Kim, M., C.V. Carman, and T.A. Springer. 2003. Bidirectional transmembrane signaling by cytoplasmic domain separation in integrins. *Science.* 301:1720–1725. doi:10.1126/science.1084174

Kirshner, J., C.J. Chen, P. Liu, J. Huang, and J.E. Shively. 2003. CEACAM1-4S, a cell-cell adhesion molecule, mediates apoptosis and reverts mammary carcinoma cells to a normal morphogenic phenotype in a 3D culture. *Proc. Natl. Acad. Sci. USA.* 100:521–526. doi:10.1073/pnas.232711199

Klaile, E., M.M. Müller, C. Kannicht, B.B. Singer, and L. Lucka. 2005. CEACAM1 functionally interacts with filamin A and exerts a dual role in the regulation of cell migration. *J. Cell Sci.* 118:5513–5524. doi:10.1242/jcs.02660

Klaile, E., O. Vorontsova, K. Sigmundsson, M.M. Müller, B.B. Singer, L.-G. Öfverstedt, S. Svensson, U. Skoglund, and B. Öbrink. 2009. The CEACAM1 N-terminal Ig domain mediates cis- and trans-binding and is essential for allosteric rearrangements of CEACAM1 microclusters. *J. Cell Biol.* 187:553–567.

Leung, N., C. Turbide, B. Balachandra, V. Marcus, and N. Beauchemin. 2008. Intestinal tumor progression is promoted by decreased apoptosis and dysregulated Wnt signaling in *Ceacam1-/-* mice. *Oncogene.* 27:4943–4953. doi:10.1038/onc.2008.136

Liu, Y., M.J. Kruhlak, J.-J. Hao, and S. Shaw. 2007. Rapid T cell receptor-mediated SHP-1 S591 phosphorylation regulates SHP-1 cellular localization and phosphatase activity. *J. Leukoc. Biol.* 82:742–751. doi:10.1189/jlb.1206736

Luo, B.H., C.V. Carman, and T.A. Springer. 2007. Structural basis of integrin regulation and signaling. *Annu. Rev. Immunol.* 25:619–647. doi:10.1146/annurev.immunol.25.022106.141618

Müller, M.M., B.B. Singer, E. Klaile, B. Öbrink, and L. Lucka. 2005. Transmembrane CEACAM1 affects integrin-dependent signaling and regulates extracellular matrix protein-specific morphology and migration of endothelial cells. *Blood.* 105:3925–3934. doi:10.1182/blood-2004-09-3618

Nagaishi, T., L. Pao, S.H. Lin, H. Iijima, A. Kaser, S.W. Qiao, Z. Chen, J. Glickman, S.M. Najjar, A. Nakajima, et al. 2006. SHP1 phosphatase-dependent T cell inhibition by CEACAM1 adhesion molecule isoforms. *Immunity.* 25:769–781. doi:10.1016/j.immuni.2006.08.026

Öbrink, B. 1997. CEA adhesion molecules: multifunctional proteins with signal-regulatory properties. *Curr. Opin. Cell Biol.* 9:616–626. doi:10.1016/S0955-0674(97)80114-7

Öbrink, B., and I. Hunter. 1998. Cell adhesion and signaling by the rodent CEA family. *In* Cell Adhesion and Communication Mediated by the CEA Family: Basic and Clinical Perspectives. C.P. Stanners, editor. Harwood Academic Publishers GmbH, Amsterdam. 73–98.

Öbrink, B., H. Sawa, I. Scheffrahn, B.B. Singer, K. Sigmundsson, U. Sundberg, R. Heymann, N. Beauchemin, G. Weng, P. Ram, and R. Iyengar. 2002. Computational analysis of isoform-specific signal regulation by CEACAM1-A cell adhesion molecule expressed in PC12 cells. *Ann. N. Y. Acad. Sci.* 971:597–607. doi:10.1111/j.1749-6632.2002.tb04536.x

Olsson, H., K. Wikström, G. Kjellström, and B. Öbrink. 1995. Cell adhesion activity of the short cytoplasmic domain isoform of C-CAM (C-CAM2) in CHO cells. *FEBS Lett.* 365:51–56. doi:10.1016/0014-5793(95)00436-D

Poole, A.W., and M.L. Jones. 2005. A SHPing tale: perspectives on the regulation of SHP-1 and SHP-2 tyrosine phosphatases by the C-terminal tail. *Cell. Signal.* 17:1323–1332. doi:10.1016/j.cellsig.2005.05.016

Sankarshanan, M., Z. Ma, T. Iype, and U. Lorenz. 2007. Identification of a novel lipid raft-targeting motif in Src homology 2-containing phosphatase 1. *J. Immunol.* 179:483–490.

Scheffrahn, I., B.B. Singer, K. Sigmundsson, L. Lucka, and B. Öbrink. 2005. Control of density-dependent, cell state-specific signal transduction by the cell adhesion molecule CEACAM1, and its influence on cell cycle regulation. *Exp. Cell Res.* 307:427–435. doi:10.1016/j.yexcr.2005.03.030

Sigmundsson, K. 2004. Characterization and modelling of CEACAM1 interactions in cell signalling. PhD thesis. Karolinska University Press, Stockholm. 115 pp.

Singer, B.B., I. Scheffrahn, and B. Öbrink. 2000. The tumor growth-inhibiting cell adhesion molecule CEACAM1 (C-CAM) is differently expressed in proliferating and quiescent epithelial cells and regulates cell proliferation. *Cancer Res.* 60:1236–1244.

Singer, B.B., I. Scheffrahn, R. Heymann, K. Sigmundsson, R. Kammerer, and B. Öbrink. 2002. Carcinoembryonic antigen-related cell adhesion molecule 1 expression and signaling in human, mouse, and rat leukocytes: evidence for replacement of the short cytoplasmic domain isoform by glycosylphosphatidylinositol-linked proteins in human leukocytes. *J. Immunol.* 168:5139–5146.

Singer, B.B., E. Klaile, I. Scheffrahn, M.M. Müller, R. Kammerer, W. Reutter, B. Öbrink, and L. Lucka. 2005. CEACAM1 (CD66a) mediates delay of spontaneous and Fas ligand-induced apoptosis in granulocytes. *Eur. J. Immunol.* 35:1949–1959. doi:10.1002/eji.200425691

Slevogt, H., S. Zabel, B. Opitz, A. Hocke, J. Eitel, P.D. N'guessan, L. Lucka, K. Riesbeck, W. Zimmermann, J. Zweigner, et al. 2008. CEACAM1 inhibits Toll-like receptor 2-triggered antibacterial responses of human pulmonary epithelial cells. *Nat. Immunol.* 9:1270–1278. doi:10.1038/ni.1661

Toyoshima, K., N. Ito, Y. Hiasa, Y. Kamamoto, and S. Makiura. 1971. Tissue culture of urinary bladder tumor induced in a rat by N-butyl-N-(-4-hydr oxybutyl)nitrosamine: establishment of cell line, Nara Bladder Tumor II. *J. Natl. Cancer Inst.* 47:979–985.

Wikström, K., G. Kjellström, and B. Öbrink. 1996. Homophilic intercellular adhesion mediated by C-CAM is due to a domain 1-domain 1 reciprocal binding. *Exp. Cell Res.* 227:360–366. doi:10.1006/excr.1996.0285

Yokoyama, S., C.J. Chen, T. Nguyen, and J.E. Shively. 2007. Role of CEACAM1 isoforms in an in vivo model of mammary morphogenesis: mutational analysis of the cytoplasmic domain of CEACAM1-4S reveals key residues involved in lumen formation. *Oncogene.* 26:7637–7646. doi:10.1038/sj.onc.1210577

Zacharias, D.A., J.D. Violin, A.C. Newton, and R.Y. Tsien. 2002. Partitioning of lipid-modified monomeric GFPs into membrane microdomains of live cells. *Science.* 296:913–916. doi:10.1126/science.1068539